npg

Pigment epithelium-derived factor expression prolongs survival and enhances the cytotoxicity of low-dose chemotherapy in castration-refractory prostate cancer

T Nelius[1], D Martinez-Marin[1], J Hirsch[1], B Miller[2], K Rinard[1], J Lopez[1], W de Riese[1] and S Filleur*,[1,3]

There is currently no cure for advanced castration-refractory prostate cancer (CRPC) despite the recent approval of several new therapeutic agents. We report here the anti-tumor effect of the angio-inhibitory pigment epithelium-derived factor (PEDF) in the metastatic LNCaP-derivative CRPC CL1 model and explore PEDF anti-neoplasic efficacy in combination with low-dose chemotherapy. Androgen-sensitive LNCaP and CRPC PC3 cell lines were examined as comparison. Using a retroviral expression system, we showed that PEDF limited the proliferation of all prostatic cell lines tested; an effect attributed to interleukin 8 (IL8)-CXCR1/IL8RA inhibition. PEDF also reduced the number and size of 3D tumor spheroids *in vitro*, but only induced cell differentiation in CRPC spheroids. Similarly, PEDF inhibited the migration of CRPC cells suggesting both anti-proliferative and anti-migratory functions. *In vivo*, PEDF decreased by 85% and 65% the growth of subcutaneous (s.c.) PC3 and CL1 tumors, respectively. In the CL1 orthotopic model, tumor intake with lethal metastases was found in all animals; nevertheless, PEDF prolonged the median survival of tumor-bearing mice (95% confidence interval: 53 ± 0.001 to 57 ± 1 days). Accordingly, PEDF delayed the emergence of skeletal-related event in intra-tibial xenografts. Next, we evaluated low-dose docetaxel (DTX; 5, 1, 0.5 mg/kg) or cyclophosphamide (CTX; 10–20 mg/kg) on established s.c. PC3 tumors that conditionally express PEDF anti-tumoral epitope/NT3. Although NT3–DTX-5 mg/kg combination was inefficient, NT3–DTX-1 mg/kg and -0.5 mg/kg inhibited by 95% and 87.8%, respectively, tumor growth compared with control and induced tumor stasis. Both NT3–CTX combinations were advantageous. Inversely, PEDF–DTX-5 mg/kg and PEDF–CTX-10 mg/kg delayed the most CL1 tumor growth (15, 11 and 5 days for PEDF–DTX-5 mg/kg, PEDF–CTX-10 mg/kg and single treatments, respectively) with elevated apoptosis and serum thrombospondin-1 as possible mechanism and marker, respectively. As well, both PEDF–CTX-10 mg/kg and PEDF–DTX-5 mg/kg prolonged significantly the survival of tumor-bearing mice compared with single treatments. Metastases were reduced in PEDF–DTX-5 mg/kg compared with other treatments, suggesting that PEDF–DTX delayed metastases formation. Our results advocate that PEDF/low-dose chemotherapy may represent a new therapeutic alternative for CRPC.

Prostate cancer continues to be the most common malignancy, excluding skin cancer, and the second leading cause of cancer-related death in men in Western countries. Although early stages of the disease are curable, metastatic castration-refractory prostate cancer (mCRPC) stages are highly aggressive and virtually incurable. Docetaxel (DTX/Taxotere)/prednisone was the first chemotherapy regimen approved by the US Food and Drug Administration that could demonstrate 2.5 months survival benefit in mCRPC patients.[1–3] Although many patients respond initially, they ultimately develop a resistance to the treatment. The rapid approval of several novel agents including

sipuleucel-T/Provenge, cabazitaxel/Jevtana, abiraterone acetate/Zytiga and MDV3100/Enzalutamide has given DTX-resistant CRPC patients additional therapeutic options, however, the overall survival benefits remain modest.[4] Therefore, new therapeutic agents and treatment strategies are still needed. Furthermore, given the toxicity of some of these treatments, a re-evaluation of the way to administer these regimens must be considered in order to improve the quality of life of mCRPC patients and further improve survival.

Pigment epithelium-derived factor (PEDF) is a 50-kDa glycoprotein that blocks angiogenesis[5] and promotes neuronal cell survival and differentiation.[6] PEDF is expressed

as a secreted factor in many tissues.[6,7] In the prostate, PEDF is, respectively, up- and downregulated after androgen-ablation therapy and in response to hypoxia. In PEDF knockout mice, a hyper-vascularization of the prostate in combination with hyperplasia was described.[8] PEDF expression has been shown to be downregulated in multiple human solid tumors, including prostate cancer.[8] Moreover, PEDF reduction in prostate cancer has been associated with poor prognosis.[8,9] In a previous study, we have re-expressed *PEDF* gene in human CRPC PC3 cells and demonstrated that this decreases tumor growth *in vivo*.[10] We also identified the N-terminal region (amino acids 1–101) as responsible for PEDF anti-tumor effect.[10] PEDF's growth inhibition was attributed to its capacity (1) to inhibit cancer cell proliferation through the reduction of interleukin-8 (IL8), a ELR + CXC chemokine that is overexpressed in CRPC and has been involved in the emergence of tumor resistance against chemotherapeutic agents;[11–13] (2) to induce cancer cell differentiation;[14] and (3) to block tumor neo-vascularization.[10,15] In addition, we and others have shown that PEDF acts directly on macrophages to induce their migration and differentiation toward a M1/tumor cytotoxic phenotype,[16,17] confirming PEDF's inflammatory role as previously described in the central nervous[18–21] and ocular systems.[22,23] Although our previous studies clearly demonstrated that PEDF has strong anti-tumor properties, further preclinical models have yet to be tested. More importantly, the significance of PEDF in combination with chemotherapy has never been studied and necessitates more investigation.

Low-dose or so-called metronomic chemotherapy protocols are characterized as frequent, regular and long-term administration of chemotherapeutic agents without any prolonged interruptions. Metronomic chemotherapies have demonstrated important stabilizing effects on cancer, including chemotherapy-resistant disease, to confer prolonged clinical benefit and to have positive effects on the quality of life of mCRPC patients, without high-grade toxicity.[24,25] Cyclophosphamide (CTX) is a nitrogen mustard alkylating agent that is used to treat various types of cancer.[26] High doses of CTX have been associated with cytotoxicity and immunosuppression.[26] In contrast, low-dose oral CTX demonstrated anti-angiogenic,[27–31] anti-vasculogenic[32] and increased anti-tumor immunity properties.[33,34] In clinical studies, oral CTX was well tolerated. It also showed an impact on prostate-specific antigen response and objective remission in CRPC patients.[35] In recent clinical trials, the CTX oral dose was lowered even further and was given on a daily basis.[26,36] Similarly, low-dose DTX is an effective and well-tolerated treatment for mCRPC,[37,38] and also enhanced the anti-tumor effects of several therapeutic agents in prostatic xenografts.[31,39–41]

In the present study, we investigated the anti-tumor properties of PEDF in an orthotopic mouse model for CRPC. In this model, we evaluated the capacity of PEDF to inhibit tumor growth, bone metastases formation and to prolong the survival of tumor-bearing mice. We have also assessed the therapeutic efficacy of PEDF in combination with low-dose CTX or DTX. Our results clearly demonstrate that PEDF expression reduced the growth of primary tumors, prolonged the survival of tumor-bearing mice and enhanced the anti-tumor efficacy of low-dose chemotherapy *in vivo*. These findings may lead to the development of new therapeutic strategies for mCRPC.

Results

PEDF expression inhibits cell proliferation, migration and spheroid formation, and stimulates the differentiation of CRPC cells *in vitro*. We recently validated the androgen-sensitive LNCaP and its CRPC derivative CL1 cells as an innovative model to study mCRPC.[42] In the present study, we therefore seek to use this model to further validate PEDF anti-tumor effects. Using a bicistronic retroviral system, we co-expressed the DsRed Express fluorescent protein with or without the human PEDF in LNCaP and CL1 cell lines. Similarly, PC3 cells were used as positive control. After transduction, DsRed Express-expressing cells were selected by fluorescence-activated cell sorting (purity > 96%). As expected, both control/Empty/E and PEDF/P sorted cell lines expressed the DsRed Express protein (Figure 1a). PEDF secretion in the cell media was verified by western blotting (Figure 1a). Cell growth and 3D spheroid formation *in vitro* assays demonstrated that PEDF expression limits significantly the proliferation of both androgen-sensitive and CRPC cells (Figure 1b). PEDF also reduced the number and size of tumor spheroids formed (Figure 1c), suggesting an anti-proliferative effect. Interestingly, while PEDF induced cell differentiation in CRPC spheroids (see dendrite-like structures in Figure 1c), no effect was seen on androgen-sensitive LNCaP cells. We previously demonstrated that PEDF inhibits the proliferation of CRPC cells through downregulation of IL8.[15] Although IL8 was not detected in LNCaP cells, it was found to be expressed in both PC3 and CL1 cells, with CL1 expressing the highest level. Surprisingly, while IL8 was downregulated in PC3 cells in response to PEDF, no effect was observed in CL1 cells (Figure 1d). We then analyzed the expression levels of IL8 receptors, CXCR1/IL8RA and CXCR2/IL8RB. Using quantitative PCR, we demonstrated that CXCR2/IL8RB mRNA is expressed at different levels in prostate cancer cells and is not regulated by PEDF (data not shown). Inversely, CXCR1/IL8RA mRNA is overexpressed in CRPC compared with androgen-sensitive cells and is strongly repressed by PEDF (Figure 1d), suggesting that IL8/CXCR1 axis is involved in PEDF-stimulated tumor cell growth inhibition. As an indication of the capacity of prostate cancer cells to migrate from the primary tumor to secondary tissue sites, we performed *in vitro* migration assays. Using gelatin-coated insert, we demonstrated that PEDF inhibited significantly the migration of PC3 and CL1 cells (Figure 1e), suggesting that PEDF curbs both the proliferation and migration of prostate cancer cells *in vitro*.

PEDF blocks tumor growth and prolongs survival in the CRPC CL1 preclinical model. To corroborate the anti-tumor properties of PEDF *in vivo*, we performed s.c. xenograft experiments using the fluorescent LNCaP, PC3 and CL1 cells that express or do not express PEDF. As expected, nude mice injected with LNCaP cells (in the absence of Matrigel) did not form any tumors
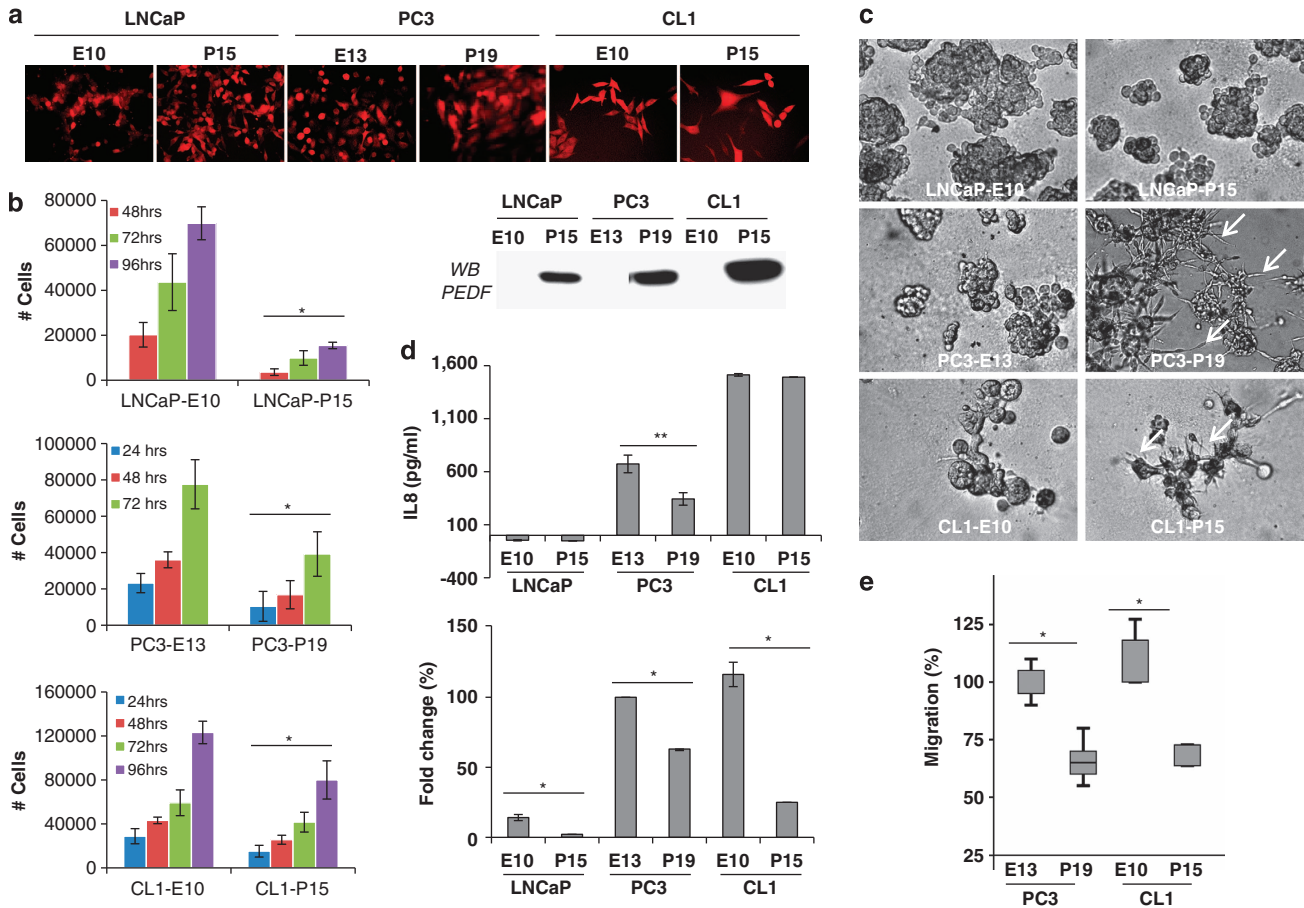
Figure 1 The effects of PEDF on the proliferation, migration, spheroids formation and IL8/CXCR1 expression by prostate cancer cells in vitro. (**a**) (Top panel) DsRed Express expression was visualized by fluorescence microscopy in all the transduced human prostate cancer cell lines tested. (Bottom panel) PEDF secretion was tested by western blotting in the corresponding cell-conditioned media. (**b**) In vitro growth curves. Prostate cancer cells were seeded in quadruplicate at 10^4 cells/well into 24-well plates. After 24, 48, 72 and 96 h, cells were trypsinized, stained with Trypan blue dye and counted. Error bars = mean ± S.E.M. (*$P < 0.05$). (**c**) 3D tumor spheroid formation in culture matrix basement membrane extract reduced growth factor was performed on tumor cells for 14 days. Note the reduced number and smaller size of the spheroids formed in the presence of PEDF. Note also the differentiation of CRPC tumor spheroids (white arrows) in response to PEDF expression. (**d**) (Top panel) IL8 production by prostate cancer cells. Tumor cell-conditioned media were collected and tested for IL8 by ELISA. Obtained values were reported to the total amount of proteins (**$P = 0.00178$). (Bottom panel) RNAs were extracted from prostate tumor cells and reverted into cDNA. cDNAs were then amplified using qPCR to measure specifically the expression level of CXCR1 (*$P < 0.05$). (**e**) In vitro migration assays. Control/E- or PEDF/P-expressing PC3 and CL1 cells were seeded on a semi-permeable membrane (8 μm size pore) and incubate overnight to allow migration. Cells that migrated were then fixed, stained and counted in 10 high-powered fields (*$P < 0.05$)

(data not shown). Although PC3 cells were tumorigenic, PEDF expression inhibited the growth of these tumors in vivo by 85% (Figure 2a). In the CL1 model, control/Empty tumors (CL1–E10) were found highly tumorigenic with tumor invasion to adjacent muscular and bone structures. In contrast, PEDF-expressing tumors (CL1–P15) were more superficial, 65% smaller and showed a significant reduction in microvessel density (Figure 2b), validating PEDF anti-tumoral and anti-angiogenic properties in the highly aggressive and metastatic CL1 model. Next, CL1–E10 or CL1–P15 cells were injected into the left lobe of the dorsal prostate of C.B.17-SCID mice. Tumor intake was 100%. All animal deaths were found concomitant to a widespread metastatic phenotype. Survival studies showed that PEDF expression prolongs significantly ($P = 0.01$; 95% confidence interval) the median survival of CL1 tumor-bearing mice (53 ± 0.001 versus 57 ± 1 days; Figure 2c). At the time of death/killing, primary tumor and metastases were assessed by in vivo

fluorescence bioimaging (Figures 2d–f). In both CL1–E10 control and CL1–P15 groups, the primary tumors and pancreas were found highly fluorescent (Figure 2d). No size differences of the primary tumors were observed between the groups (data not shown). Fluorescence was also detected in the testes, seminal vesicles, lung, kidney, liver, heart, lymph nodes, tibia and spine (Figures 2e and f) of both groups, suggesting that primary tumors spread to multiple distant organs/sites causing the death of the animals. Histopathological analyses confirmed the highest grade of both control and PEDF-expressing primary tumors (Gleason grade: $5 + 5$) with anaplastic/pleiomorphic features, extensive geographic tumor necrosis and lymphovascular invasion. The presence of numerous metastases was also confirmed. Metastases were found in nodules in the pancreas, liver, lymph nodes and lung. Inversely, tumors were found to be non-invading in the testis, kidney, vertebral column and tibia (Figures 2g–l). In summary, we demonstrated
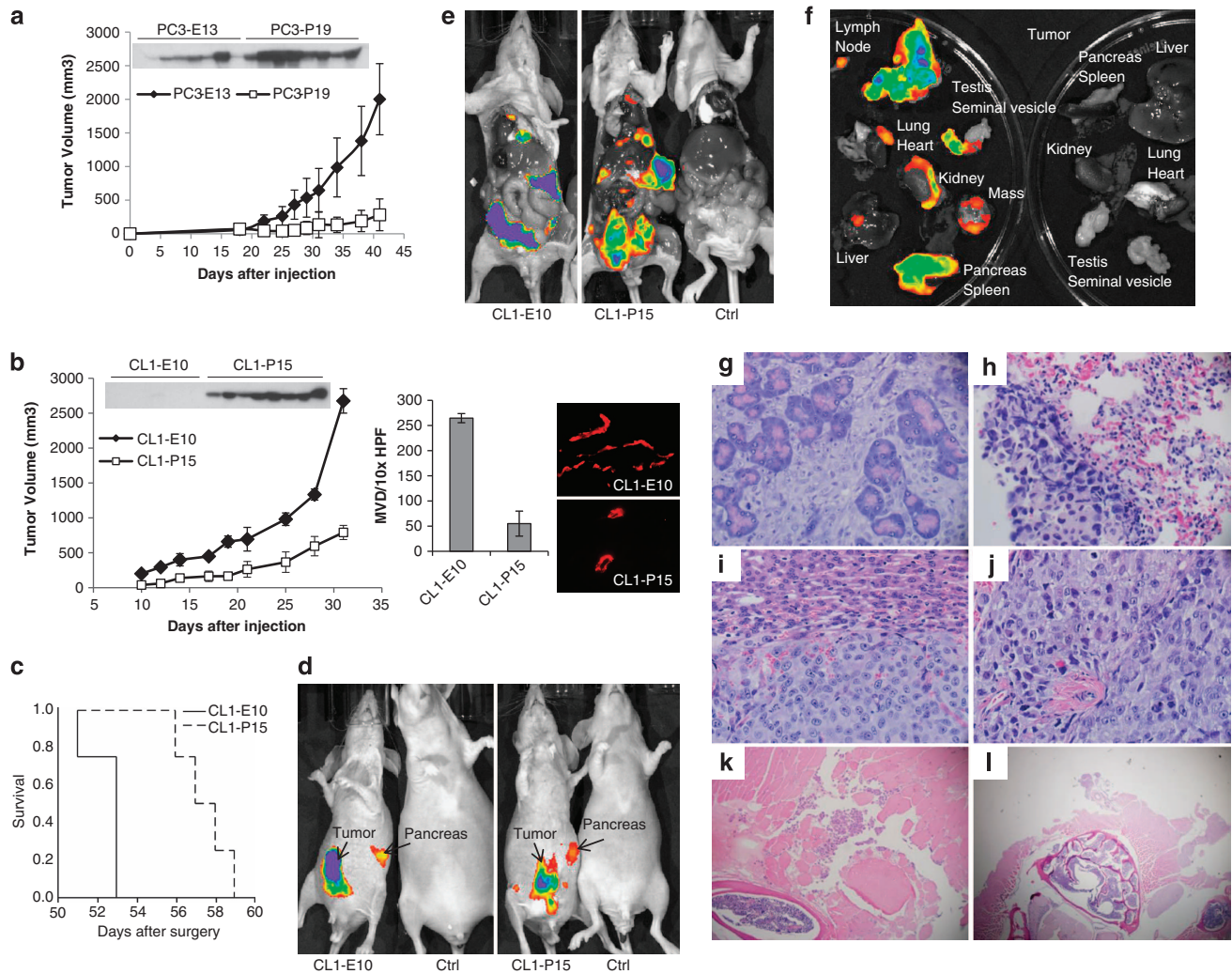
Figure 2 PEDF expression inhibits tumor growth and prolongs survival in CL1 xenografts. The CL1 cells that co-express the DsRed express fluorescent protein with PEDF (CL1–P15) or control empty plasmid (CL1–E10) were used as *in vivo* model to test the effect of PEDF expression on tumor growth (**b**) and on the survival of tumor-bearing mice (**c**). As positive controls, PC3 cells that co-express the DsRed Express protein with (PC3-P19) or without (PC3-E10) PEDF were used (**a**). Tumor volumes were measured twice a week for ~40 days. At the end point of the experiment (day 42 for PC3 tumors and day 32 for CL1 tumors), mice were killed, blood was collected from the heart, serum was then prepared and tested for PEDF by western blotting (**a** and **b**; top panels). It is to note that PEDF was detected in the serum of mice bearing PC3 control tumors, whereas absent in CL1 control mice, suggesting that the host PEDF expression level may encounter for at least part of the difference in aggressiveness observed between the two models tested. Tumors were collected and then were frozen for microvessel density staining (CD31 staining, (**b**) right panel). (**c**) Survival study. CL1–E10 or CL1–PEDF cells were injected into the prostate gland of anesthetized CB17-SCID mice. Survival analyses were carried out using the Kaplan–Meier curves and the log rank test. At the end point of the experiment (time of death), DsRed Express fluorescent protein was visualized by *in vivo* fluorescence imaging on total (**d**; CL1–E10/tumor-free control (left) and CL1–PEDF/ tumor-free control (right)), opened mice (**e**; CL1–E10/CL1–PEDF/tumor-free control) and isolated organs (**f**; CL1–PEDF/tumor-free control). (**g–l**) Histopathology analyses (×10 magnification) showing tumor invasion to the pancreas (**g**), lung (**h**), liver (**i**), lymph nodes (**j**) the paraspinal musculature (**k**) and lymphovascular spinal area (**l**) in CL1–PEDF animal group. Please note the absence of differences in metastasis distribution and tissue invasion between the CL1–E10 and CL1–PEDF groups

that PEDF inhibits the growth of s.c. PC3 and CL1 prostatic tumors and prolongs the survival of tumor-bearing mice in the CL1 orthotopic model.

PEDF expression curbs metastases formation and bone destruction in the CL1 intra-tibial model. To determine whether PEDF may limit the formation of bone metastases, a common and problematic site of metastasis in mCRPC, CL1 cells were injected into the proximal region of mice tibia. The occurrence of skeletal-related events (SREs) (Figure 3a) as defined by appearance of clinical signs, such as problem

walking/limping in combination with the presence of osteolytic lesion/pathologic bone fractures and a positive signal as measured by *in vivo* X-ray/fluorescence imaging (Figure 3b), was then assessed. With this end point, we were able to demonstrate that PEDF delayed significantly the emergence of SRE (39.4 ± 2.421 *versus* 51 ± 2.5777 days; $P = 0.008$). At the time of the imaging, both CL1–E10 and CL1–P15 fluorescent tumor cells were found in the bone and resulted in the formation of osteolytic lesions (Figures 3b, d and e). Because of their high level of aggressiveness, tumor cells were also found in the surrounding muscles (Figures 3c–i).
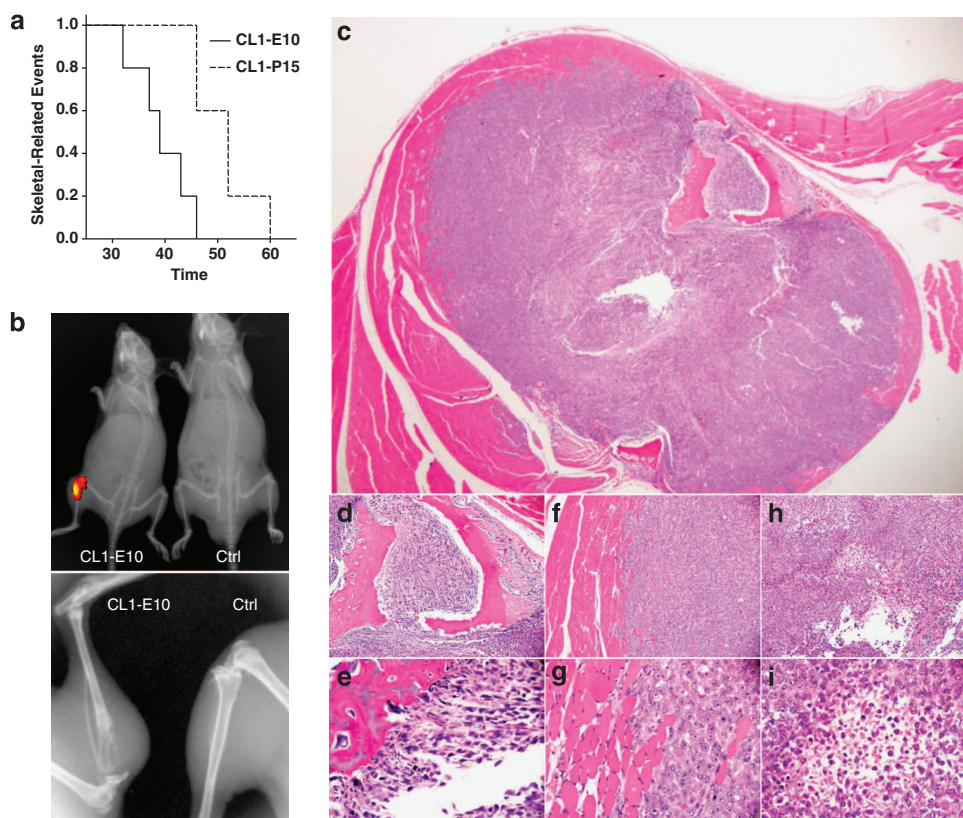
Figure 3 PEDF effect on SREs. (**a**) PEDF delays the occurrence of SREs *in vivo*. CL1–E10 or CL1–P15 cells were injected into the tibia of anesthetized CB17-SCID mice. The appearance of SREs was observed overtime (**a**) and defined as a combination of clinical signs (severe limping) with significant fluorescent signal due to tumor (**b**, top panel, overlay fluorescence/X-ray) and osteolytic lesion in the bone (**b**, bottom panel, X-ray) with fractures. After killing, mice tibias surrounded by muscles were collected, and were subsequently decalcified, fixed in formalin, embedded in paraffin and sectioned for H&E analysis. (**c–i**) Histopathology showing an overview of tumor cells (**c, h** and **i**) inside the bone (**c–e**) and invading the surrounding muscle (**c, f–g**) of a CL1–E10 mouse. (**c**) × 4 magnification; (**d, f, h**); × 10 magnification; (**e, g, i**) × 40 magnification

PEDF expression and low-dose chemotherapy curbed PC3 and CL1 s.c. tumor growth. Low-dose chemotherapy has shown great promise when combined with targeted anti-angiogenic factors.[31,43,44] Other investigators emphasized on IL8 as key modulator of resistance against conventional chemotherapeutic drugs such as DTX.[45] We therefore hypothesized that PEDF may enhance the cytotoxicity effects of low-dose chemotherapies in CRPC. To test this hypothesis, we used PC3 inducible cells for the anti-tumoral N terminus fragment of PEDF as preclinical model.[10] Once tumors reached a size of $\sim 90\,mm^3$, mice received doxycycline (Dox) or carrier to induce or block PEDF N-terminal expression (NT3), respectively, and underwent low doses of DTX (5, 1 and 0.5 mg/kg), CTX (10 and 20 mg/kg) or placebo (Figure 4a and Supplementary Table 1). All treatments were well tolerated and no side effects were observed. All single treatments markedly inhibited tumor growth compared with controls (Figure 4 and Supplementary Table 1). Dox treatment in mice injected with PC3 empty plasmid did not show any effects on tumor growth (data not shown). In the combined treatments, while NT3–DTX-5 mg/kg did not exhibit any significant effects compared with PEDF group (Figure 4b and Supplementary Table 1), NT3–DTX-1 mg/kg inhibited by 95% tumor growth compared with control and induced the stasis of PC3 tumors compared with single

treatments (Figure 4c). Similarly, NT3–DTX-0.5 mg/kg was inhibitory (Figure 4d); however, the effects were lesser than NT3–DTX-1 mg/kg (treatment/control (T/C)%: 4.9 *versus* 12.2 for NT3–DTX-1 mg/kg and NT3–DTX-0.5 mg/kg, respectively). For CTX, while CTX-20 mg/kg was found more effective than CTX-10 mg/kg in monotherapy (T/C%: 11.98 *versus* 21.25 for CTX-20 mg/kg and CTX-10 mg/kg, respectively), both NT3–CTX combined regimens showed similar additive inhibitory effects (Figures 4e and f). In the CL1 model (Figure 5), all the single treatments tested delayed tumor growth by up to 5.5 days compared with the control/untreated group (Supplementary Table 2). Delays in tumor growth were further increased for all combinations (15, 11, 9, 11 and 8 days or 15.2, 23.3, 28, 25 and 36.4 T/C% for PEDF combined with DTX-5 mg/kg, -1 mg/kg and -0.5 mg/kg; and CTX-10 mg/kg and -20 mg/kg, respectively), with PEDF-DTX-5 mg/kg and PEDF–CTX-10 mg/kg being the most efficient regimens (Figures 5a and b). All the differences were highly significant. To understand the anti-tumor mechanisms involved, we investigated cleaved PARP as a marker of apoptosis in cultured CRPC cells. Although PC3 cells were found to be resistant to both DTX and CTX, apoptosis was moderately induced (up to 36%) in CL1 cells undergoing combined treatments (data not shown), suggesting that apoptosis may have a secondary role. Thrombospondin-1
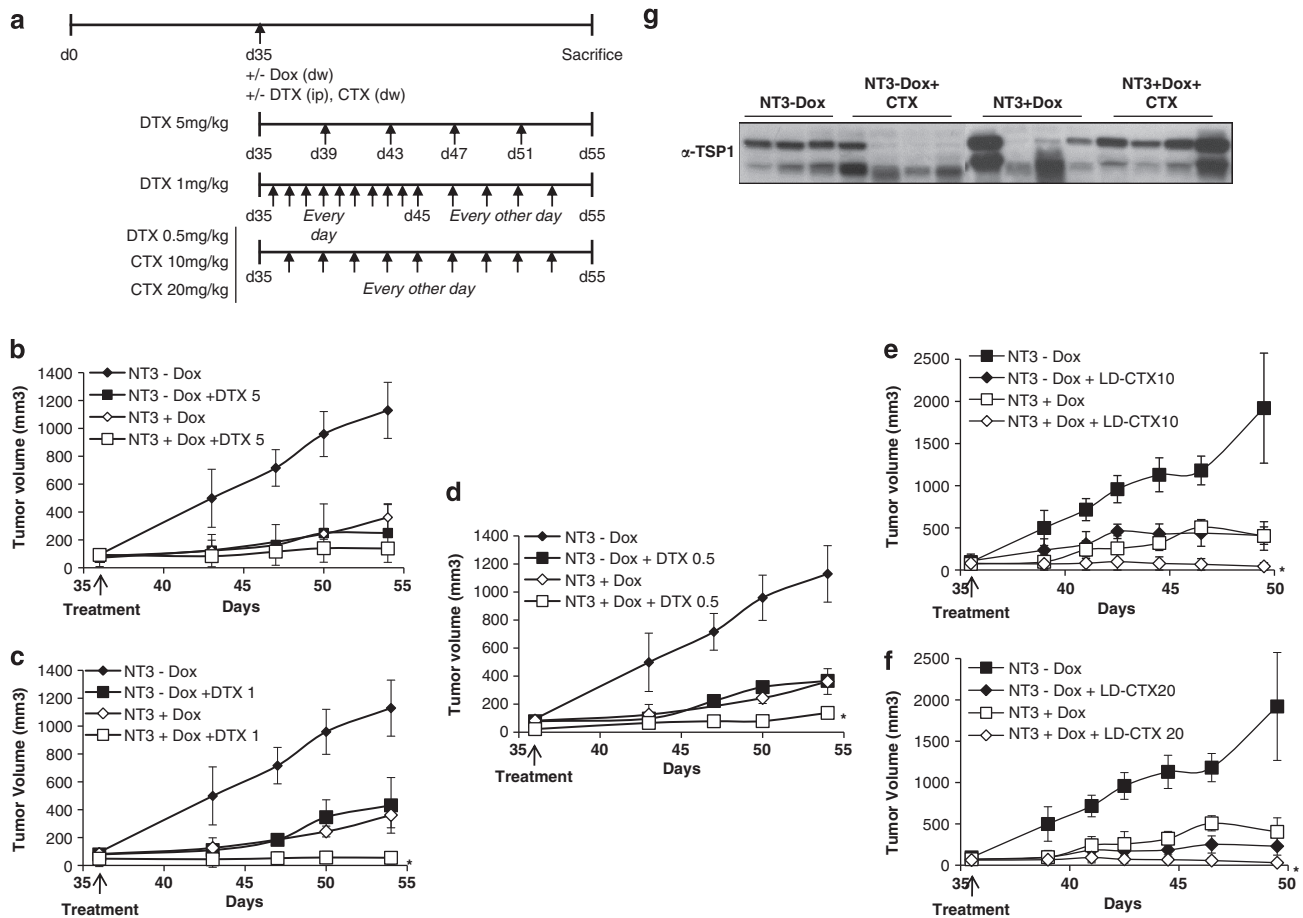
Figure 4 Anti-tumor effect of PEDF and low-dose chemotherapy on PC3 tumors. (**a**) Treatment schedule for the tetracycline-inducible PC3 *in vivo* model for PEDF N terminus. (**b**–**f**) PC3 tumor growth in mice undergoing PEDF N terminus and low-dose chemotherapy combined treatment. 1×10^6 PC3 cells were injected s.c. into the hindquarters of Nu/Nu mice. Once tumors reached an average size of $\sim 90\,mm^3$ (day 35), mice were randomized and received Dox or carrier to induce or block the expression of PEDF N terminal with either 5 mg/kg DTX (i.p., every 4 days; **b**), 1 mg/kg DTX (i.p., every day for 10 days, then every other day; **c**), 0.5 mg/kg DTX (i.p., every other day; **d**), 10 mg/kg CTX (in the drinking water, **e**), 20 mg/kg CTX (in the drinking water, **f**) or placebo. Tumors were measured twice a week for ~ 20 days. At the end point of the experiment, mice were killed, blood was collected from the heart, sera were isolated, serum protein concentration was determined and TSP1 secretion in the serum was measured by western blotting (**g**)

(TSP1) expression was also assessed in the serum of tumor-bearing mice. No differences were seen in DTX ± PEDF regimens (data not shown). In contrast, while PEDF expression increased TSP1 production slightly (Figures 4g–5c), PEDF/CTX treatment significantly induced TSP1, suggesting that TSP1 could act in concert with PEDF to curb tumor growth.

PEDF expression and low-dose chemotherapy prolonged survival of CL1 tumor-bearing mice. To determine whether the previous anti-tumor effects could translate into survival effects, CL1–P15 or control cells were injected orthotopically. After 1 week, animals were treated with DTX-5 m/kg, CTX-10 mg/kg (most efficient doses, Figure 5) or placebo and then followed for survival. As previously observed, PEDF prolonged the survival of tumor-bearing mice (Figure 6; 50 ± 0.00 *versus* 54 ± 0.77 days; $P = 0.0015$; 95% confidence interval). As well, CTX single treatment prolongs significantly ($P = 0.031$) the median survival of CL1 tumor-bearing mice (57 ± 0.00 days for CTX *versus* 50 ± 0.00 days for CL1 control). Interestingly, while CTX prolonged

survival with a greater extent than PEDF alone, combined treatment was more efficient (54 ± 0.77 *versus* 59 ± 2.04; $P = 0.0011$). Bioimaging did not show any size differences in the primary tumors between control, single or combined treatments (at the time of animal death/killing). Histopathology confirmed metastatic profiles similar to the ones we previously observed (Figures 3g–l). As CTX, DTX single treatment prolonged significantly ($P = 0.0148$) the median survival of CL1 tumor-bearing mice (91 ± 1.3 for DTX *versus* 50 ± 0.00 for control). DTX also prolonged by more than 35 days survival compared with PEDF-treated mice ($P = 0.0067$). Most importantly, PEDF/DTX prolonged with a greater extent mouse survival. In this group, 50% of the animals were still alive after 126 days (Figure 6). In these mice, whereas tumors were initially palpable, no fluorescence or tumor cells could be identified by *in vivo* imaging and histopathology, suggesting a complete tumor regression after treatment. In all the remaining DTX-treated tumor-bearing mice, the primary tumors were extremely bloody and had a similar size. However, the metastatic profiles between DTX single and PEDF/DTX combined treatments were
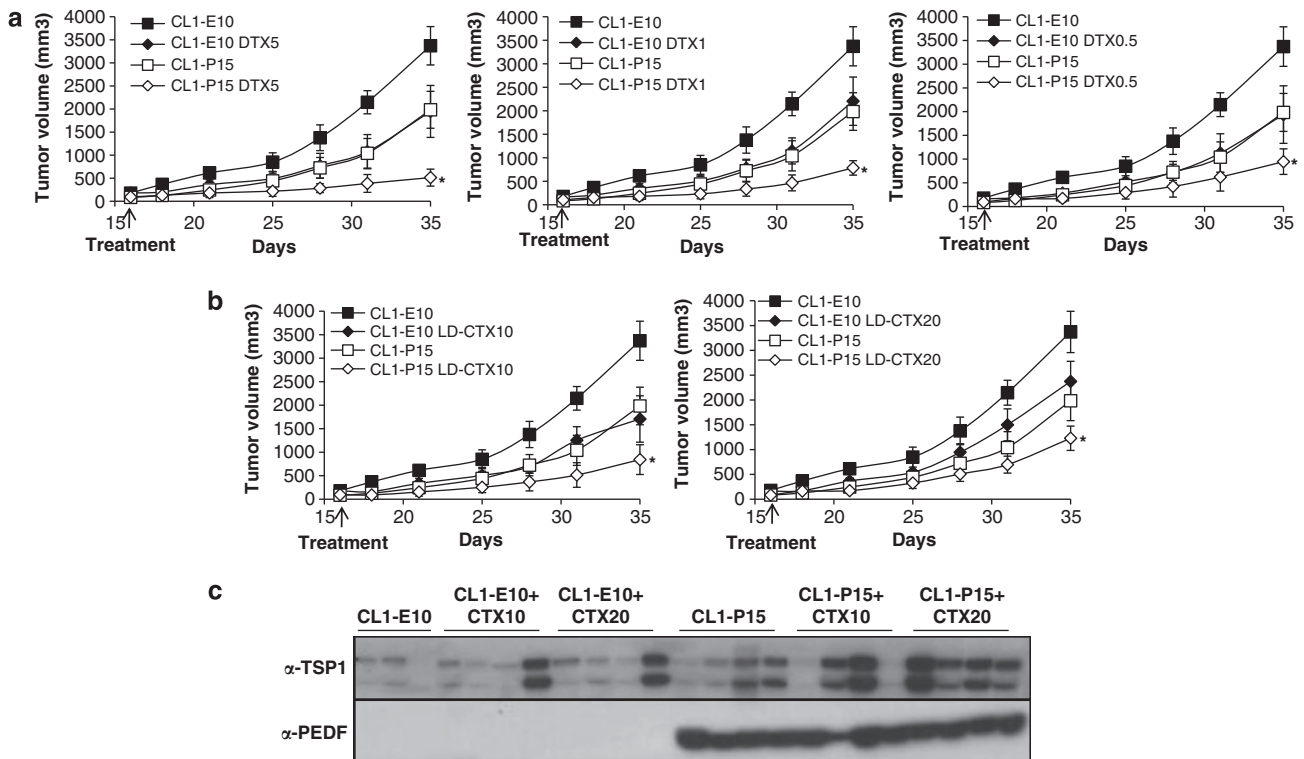
Figure 5 Anti-tumor effect of PEDF and low-dose chemotherapy on CL1 tumors. 1×10^6 CL1 cells were injected s.c. into the hindquarters of C.B.17-SCID mice. Once tumors reached an average size of $150 \pm 70/90 \pm 52\ mm^3$ (CL1–E10/CL1–PEDF; day 15), mice received DTX (5 mg/kg i.p., every 4 days; 1 mg/kg i.p., every day for 10 days, then every other day; and 0.5 mg/kg i.p., every other day; **a**); CTX (10 mg/kg and 20 mg/kg in the drinking water; **b**); or placebo. Tumors were measured twice a week for ~ 20 days. At the end point of the experiment, mice were killed, blood was collected from the heart, sera were isolated, serum protein concentration was determined and TSP1 secretion levels were measured in the serum by western blotting (**c**). $*P < 0.05$
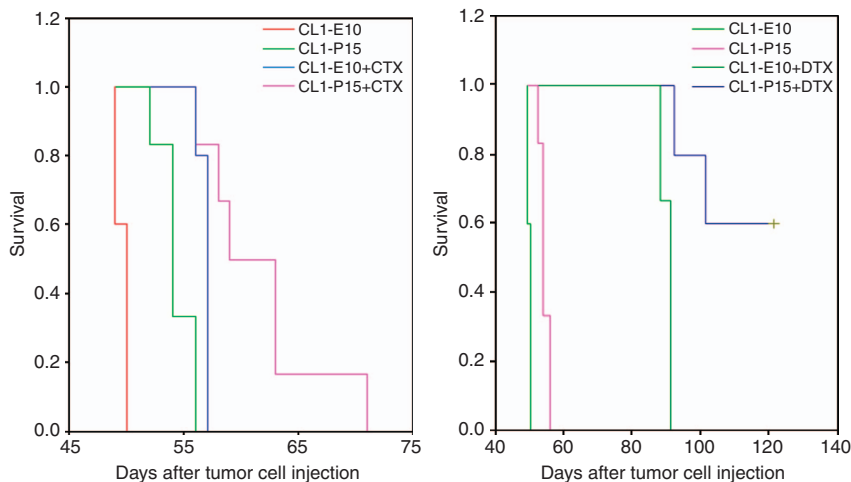

Figure 6 Survival effect of PEDF and low-dose chemotherapy combined treatment. CL1–E10 or CL1–PEDF cells were injected into the prostate gland of anesthetized CB17-SCID mice. After 1 week, mice received either 5 mg/kg DTX i.p., 10 mg/kg CTX in the drinking water or placebo. Survival analyses were carried out using the Kaplan–Meier curves and the log rank test

different. DTX group did not present metastases in the liver in contrast to the control. In addition, metastases were absent in the liver, heart and lungs of the combined treatment group. These data suggest therefore that low-dose DTX-5 mg/kg limits the formation of metastases, and that PEDF enhances DTX anti-metastatic properties.

Discussion

Despite the recent approval of several new therapeutic agents for CRPC, their overall survival effects still remain modest and their side effects are often not suitable for the treatment of elderly patients.[46–48] Although PEDF is a natural and widely

expressed factor, its known role as one of the most potent angio-inhibitor strengthened its potential use as a safe anti-cancer therapeutic agent. In a previous work, we have demonstrated that the re-expression of PEDF in CRPC PC3 inhibits tumor growth *in vivo*.[10] We have also characterized at least two anti-tumor activities for PEDF, that is, anti-angiogenic and pro-differentiative.[14] More recently, we and others have shown that PEDF inhibited the proliferation of prostate tumor cells through repression of the inflammatory chemokine IL8 and induced differentiation of macrophages toward a tumor-cytotoxic phenotype, suggesting two new mechanisms by which PEDF may inhibit indirectly tumor growth.[15–17] In the present study, we have further investigated PEDF in the mouse CL1 model for mCRPC. In this model and similar to PC3 cells, we have shown that PEDF inhibits the proliferation and migration of CL1 cells and the formation of 3D tumor spheroids *in vitro*. As well, we investigated IL8 downregulation in response to PEDF. Although IL8 was found repressed by PEDF in PC3 cells, no effect was seen in CL1 cells. In contrast, the IL8 receptor CXCR1, but not the IL8 receptor CXCR2, was inhibited by > 75% in response to PEDF, suggesting that IL8 signaling may also be involved in PEDF growth inhibitory action on CL1 cells. Although IL8 has been described as a key modulator of cell proliferation, survival, angiogenesis and cell migration, its specific role in PEDF-stimulated *in vivo* anti-tumoral function still needs further investigation. It is interesting to note that increased expression of IL8 and/or its receptors has been character-ized in cancer cells, endothelial cells, infiltrating neutrophils and tumor-associated macrophages, suggesting that IL8 may function as a significant regulatory factor within the tumor microenvironment.[49] We could therefore imagine that in addition to its direct effects on the different cell populations present in the tumor microenvironment, PEDF could indirectly curb tumor growth by inhibiting the local production of IL8.

To our knowledge, this is the first study investigating PEDF in combination with low-dose DTX or CTX in CRPC. Our data clearly demonstrated that PEDF enhances the anti-tumor efficacy of low-dose chemotherapy in s.c. and orthotopic xenografts confirming previous works of others and showing that low-dose chemotherapy regimens are more potent when combined with targeted anti-angiogenic factors.[31,39,43,44] No toxicity due to treatment was ever detected. Although Kerbel's group demonstrated the safety of low-dose CTX in drinking water,[50] the same group found intestinal toxicity for low-dose DTX (i.p. DTX-10 mg/kg, biweekly) in PC3 tumor-bearing mice.[51] As well, i.v. DTX-10 mg/kg once a week showed inconsistent toxicity, suggesting that DTX dose need to be further decreased.[39,52] In our study, lower doses for DTX (5, 1 and 0.5 mg/kg corresponding, respectively to a total dose of 25, 15 and 5 mg/kg *versus* 60 mg/kg) were tested. Similar to biweekly DTX-10 mg/kg, all our single doses inhibited significantly the growth of PC3 tumors *in vivo*. In the combined treatment, while PEDF-DTX-5 mg/kg was not superior to each single treatment alone, both DTX-1 and -0.5 mg/kg inhibited tumor growth when combined with PEDF emphasizing on the fact that total delivered dose and drug schedule need to be precisely assessed for any new therapeutic combination. Jia and Waxman[53] recently investigated PEDF and low-dose

CTX combination in colon tumors. In their *in vivo* study, mice were treated with 140 mg/kg CTX (i.p. every 6 days) while we used 10–20 mg/kg CTX (continuous delivery). Interestingly, while a 6-day repeating low-dose schedule only induced a modest regression of PC3 tumors *in vivo*, we showed that daily-delivered CTX inhibited by up to 80% tumor growth. Again this effect was further increased by PEDF expression. Similar to the PC3 model, PEDF enhanced the anti-tumor effects of low-dose DTX and CTX on CL1 s.c. tumors with the highest effects found for DTX-5 mg/kg and CTX-10 mg/kg. The molecular mechanisms involved in the combined regimen still remains partially characterized. Although PC3 cells were resistant to both chemotherapeutic drugs *in vitro*, apoptosis was slightly increased in CL1 cells, suggesting an indirect anti-tumor effect. Plasma TSP1 was also assessed. DTX did not show any effects. In contrast, TSP1 was found increased by either PEDF or PEDF–CTX combination. Our results confirm the studies of Bocci *et al.*[28] and Damber *et al.*[29] The origin of TSP1 is still unknown. In their study, Bocci demonstrated that TSP1 expression is increased in micro- and macro-vascular cells treated with low-dose CTX, while limited and unchanged in tumor cells. Involvement of activated platelets is still possible; however, *in vivo* studies remain difficult as antibodies differentiating human from mouse TSP1 are currently unavailable.

Similar to PC3 and CL1 s.c. models, we were able to demonstrate that both single CTX-10 mg/kg and combined PEDF–CTX-10 mg/kg treatments improved the survival of CL1 tumor-bearing mice compared with control and single treatment groups, respectively. Surprisingly, while we identi-fied PEDF anti-proliferative and anti-migratory effects *in vitro*, no differences in primary tumor size and metastatic profile were observed between these different groups that could be explained by the collection of the tumor/metastases at a late stage and the highly aggressiveness of CL1 cells. Interest-ingly, DTX-5 mg/kg treatment was more efficient than CTX-based regimen. Whereas DTX-5 mg/kg single therapy improved survival by > 35 days compared with PEDF group, half of the mice treated with PEDF-DTX combination were still alive after 126 days. In these mice, no tumors/metastases could be found, suggesting a complete tumor regression. In the remaining mice, imaging and histopathology showed the absence of metastases in the liver, heart and lungs. This anti-metastatic effect was increased compared with DTX single treatment that showed only absence of liver metastasis, suggesting therefore that PEDF enhanced DTX-induced anti-metastatic effect. These data also suggest that PEDF may present intrinsic anti-metastatic properties in CRPC as previously described in lung cancer, pancreatic adeno-carcinoma, osteosarcoma and melanoma.[54–57]

Taken together, our data demonstrate that PEDF inhibits the proliferation, tumor spheroid formation and migration of CRPC CL1 cells *in vitro*, and curbs tumor growth, bone metastases and prolongs survival of tumor-bearing mice in the same *in vivo* model, validating therefore PEDF anti-tumor properties in a highly metastatic CRPC model. The data of this study also show that PEDF enhances the therapeutic efficacy of low-dose chemotherapy, implicating that PEDF/low-dose chemotherapy combination might represent a safe and efficient treatment option for patients with mCRPC.

Materials and Methods

Cells and reagents. The parental androgen-sensitive LNCaP and androgen-refractory/CRPC PC3 cells were purchased from the American Type Culture Collection (Manassas, VA, USA) and were grown in RPMI1640 with 10% heat-inactivated fetal bovine serum. CRPC PC3 tetracycline-inducible cell lines (NT3) were grown as we described in the study by Filleur et al.[10] CL1 cell line, which was derived from the parental androgen-sensitive LNCaP cells grown under androgen deprivation, was a kind gift from Dr. Arie Belldegrun (University of California, Los Angeles, CA, USA). CL1 cells were grown, between passages 4 and 12, in RPMI1640 supplemented with 5% heat-inactivated charcoal–dextran-treated serum (androgen deprivation), 2 mM L-glutamine, 1 × non-essential amino acids and 1 mM sodium pyruvate as described in the study by Tso et al.[58] LNCaP cells are androgen-sensitive, tumorigenic and non-metastatic. In contrast, CL1 cells are androgen-refractory/CRPC, showed high tumorigenicity and spontaneously metastasize after orthotopic injection. As observed in CRPC patients, CL1 cells express androgen receptors but lost transcriptional regulation of prostate-specific genes in response to the androgen deprivation. Thus, LNCaP and CL1 cells represent an excellent experimental model to study mCRPC. Retropack PT67 cell line is an NIH 3T3-derived cell line designed for the production of infectious, replication-incompetent virus (Clontech, Mountain View, CA, USA). PT67 contains the Moloney murine leukemia virus (MoMuLV) gag, pol and env (10A1-derived) genes. PT67 cells were maintained in DMEM with 10% heat-inactivated fetal bovine serum, 4 mM L-glutamine and 1 mM sodium pyruvate. DTX and CTX were kindly provided by Dr. Everardo Cobos (Southwest Cancer Treatment and Research Center, Lubbock, TX, USA). CTX was reconstituted as described in the study by Man et al.[44]

Retroviral vector design and production. The human PEDF cDNA (NotI/ClaI) was cloned into the retroviral bicistronic pRetroX-IRES-DsRed Express plasmid (Clontech). PT67 cells were co-transfected with 1 μg pPUR (Clontech) and 10 μg of either pRetroX-IRES-DsRed Express or pRetroX-PEDF-IRES-DsRed Express using the Lipofectamine LTX kit (Invitrogen, Carlsbad, CA, USA). Transfectant single clones were selected in 3 μg/ml puromycin. Viral titration was determined using the Retro-X qRT-PCR titration kit (Clontech).

Generation of PEDF overexpressing prostate cancer cells. The day before the infection, cancer cells were seeded in six-well plate at 0.25×10^5 cells/well. At the time of the infection, viral supernatants were collected, filtered, combined to 4 μg/μl polybrene and incubated with cancer cells for two cycles of 12 h. Transduced prostate cancer cells (DsRed Express fluorescent protein, whole, uncloned population) were selected by fluorescence-activated cell sorting (BD FACS Aria flow cytometer; BD Biosciences, San Jose, CA, USA) to reach a purity of 96–99%. All post-sorted cell lines (LNCaP, PC3 and CL1) were then designated as –E or –P for either the Empty-DsRed Express or the PEDF-DsRed Express construct, respectively, followed by the number of the clone. The expression of the DsRed Express fluorescent protein was verified by fluorescence microscopy. As expected, both Empty/control and PEDF-expressing cell lines express the DsRed Express with a similar intensity (bicistronic mRNA). PEDF secretion was analyzed in conditioned media by western blotting using anti-PEDF antibody (Millipore, Temecula, CA, USA).

Cell growth assay. Cells were seeded at 10^4 cells per well into 24-well plates. After seeding (day 1), starting from the second day until the fifth day, cells were every day trypsinized, stained with Trypan blue dye and counted using an hemocytometer chamber.

3D tumor spheroids formation. 3D tumor spheroids formation was performed using the 3D Culture Matrix Basement Membrane Extract Reduced Growth Factor (Trevigen, Gaithersburg, MD, USA). 1×10^4 cells/ml were diluted in 24 ml of assay medium (98 ml of growth media plus 2 ml of 3D Culture Matrix RGF BME). Cell suspension (500 μl) were then added to each well of a 48-well plate pre-coated with 3D Culture Matrix RGF BME. Cell growth and structure formation were observed every day using an inverted microscope. The medium was changed every 3 days.

Cell-conditioned media. Eighty percent confluent prostate cancer cells were washed for 5 h in serum-free medium and then replenished with fresh serum-free medium as we described in the study by Filleur et al.[10] After 48 h,

cell-conditioned media were collected and centrifuged (960 r.p.m. for 10 min followed by 4000 r.p.m. for 20 min at 4 °C) to remove cell debris.

ELISA. IL8 was measured in cell-conditioned media using the human IL8 Quantikine ELISA kit (R&D Systems, Minneapolis, MN, USA).

RNA extraction and qPCR. Total RNAs were extracted using the RNeasy extraction kit (Qiagen, Valencia, CA, USA) and then converted into cDNA (Verso cDNA kit; Thermo Scientific, Pittsburgh, PA, USA) as we described in the study by Hirsch et al.[15] cDNA was amplified (RT-SYBR Green PCR Master Mix) in an MyIQ amplifier (Bio-Rad, Hercules, CA, USA): 1 × heating for 10 min at 95 °C; 40 × denaturing for 15 s at 95 °C, followed by annealing/extension, 30 s at 60 °C/30 s at 58 °C for CXCR1 or 56 °C for CXCR2 as we previously described in the study by Hirsch et al.[15] As reference, the housekeeping gene β-actin was amplified; cycle threshold (C_t) values were determined by automated threshold analysis with MyIQ version 1.0 software (Bio-Rad). The fold change for each gene was calculated using the $\Delta\Delta C_t$ method. Each sample was tested in triplicate. Real-time PCR amplicons were run on a 2% agarose gel to verify correct sizes.

***In vitro* migration assay.** In vitro migration assay was performed as we described in the study by Nellius et al.[16] with few minor modifications. 1.5×10^6 cells/ml were seeded on top of the gelatinized microporous membrane (8-mm pore size Corning insert). After 2 h, serum-free media was added to the bottom part of the well and incubated at 37 °C overnight. Migrated cells were visualized using the Diff-Quick staining kit (Dade Behring, Deerfield, IL, USA) and counted in 10 high-powered fields (× 60).

Western blotting. Sera of tumor-bearing mice were separated by 4–15% SDS-PAGE and transferred onto PVDF membrane. After blocking in TBST (10 ml Tris-base, 100 ml NaCl and 0.1% Tween 20 (pH 7.5)) containing 5% nonfat dry milk, the membranes were exposed to anti-PEDF or anti-TSP1 (Neomarkers, Fremont, CA, USA) and horseradish peroxidase-conjugated secondary Ab, and developed by chemiluminescence (ECL kit; Amersham, Pittsburgh, PA, USA). Protein loading was controlled by staining the gels with Brilliant Blue G—Colloidal Concentrate (Sigma, St. Louis, MO, USA).

Tumorigenicity assays

For s.c. tumors: 1×10^6 PC3-E13 or PC3-P19 cancer cells were injected s.c. into the hindquarters of Nu/Nu male mice (6–8 weeks, Charles River, Wilmington, MA, USA; 10 mice/group). For the CL1 s.c. model, 1×10^6 CL1–E10 or CL1–P15 cancer cells were injected s.c. into the hindquarters of C.B.17-SCID male mice (6–8 weeks, Charles River, 10 mice/group). Tumors were measured using a caliper every 5 days, for $\sim$30–40 days; the volume calculated as length × width^2 × 0.52. At the end point of the experiment (day 42 for PC3 tumors and day 32 for CL1 tumors), tumors were collected, half were fixed in formalin and embedded in paraffin for H&E staining. The other half of the tumors was frozen in OCT freezing medium. Cryosections (5 μm thick) were then prepared for CD31 immunofluorescence staining (microvessel density quantification).

For the combined treatments: 1×10^6 PC3–NT3 tetracycline-inducible cancer cells were injected s.c. into the hindquarters of Nu/Nu male mice (6–8 weeks, Charles River, 10 mice/group) as we previously described in the study by Filleur et al.[10] When tumors reached an average volume of 90 mm^3 (day 35 after tumor cells injection), mice were randomized into groups and treatment began and continued for $\sim$20 days (Figure 4a). For inducible expression, Dox in drinking water (1 mg/ml) was given to half of the animals. In addition, animals received DTX-5 mg/kg (i.p. every 4 days), DTX-1 mg/kg (i.p. every day for 10 days followed by every other day), DTX-0.5 mg/kg (i.p. every other day), CTX-10 mg/kg (0.66 ml of the CTX stock solution in 200 ml water bottle), CTX-20 mg/kg (1.25 ml of the CTX stock solution in 200 ml water bottle) or placebo (normal saline). For the CL1 model, 1×10^6 CL1–E10 or CL1–P15 cancer cells were injected s.c. into the hindquarters of C.B.17-SCID male mice (6–8 weeks, Charles River, 10 mice/group). When tumors reached an average volume of $150 \pm 70/90 \pm 52$ mm^3 (CL1–E10/CL1–PEDF; day 15 after tumor cells injection), mice were randomized into groups and treatment began (DTX-5 mg/kg, DTX-1 mg/kg and DTX-0.5 mg/kg; CTX-10 mg/kg, CTX-20 mg/kg or placebo) and continued for $\sim$20 days. Mice were weighted once a week to verify the absence of cytotoxicity related to the drug.

Tumors were measured using a caliper every 5 days, for ~20 days; the volume calculated as length $\times$ width^2 $\times$ 0.52. Tumor growth delay was calculated as the difference in median time to reach a tumor volume of 500 mm^3 for control and actively treated animals.[59] The ratio between specific T/C% groups[60] was calculated by using the median tumor volume in the treated group (T) and in the control group (C) at the end point of the experiments (day 49 or 54 for the PC3 tumors and day 35 for the CL1 tumors).

For orthotopic tumors: 1×10^5 CL1–E10 or CL1–P15 cells were injected into the left lobe of the dorsal prostate of anesthetized (80 mg/kg pentobarbital) C.B.17-SCID male hairless mice (8 mice/group). One week after surgery, animals received the chemotherapy regimens. DTX-5 mg/kg-treated groups received seven cycles every 4 days of DTX-5 mg/kg followed by six cycles every 8 days of DTX-5 mg/kg. Survival analyses were carried out using the Kaplan–Meier curves and the log rank test. Primary tumors and metastases were monitored at the time of the mouse killing by total and opened fluorescence imaging to visualize the DsRed Express fluorescent protein using the bioluminescence IVIS Lumina II XR animal imaging system (Caliper, Hopkinton, MA, USA). For fluorescence imaging, animals were anesthetized by isoflurane inhalation and maintained on 3% isoflurane in oxygen delivered through nose cones on a manifold in a vaporization-type anesthesia device (Caliper). As negative control, tumor-free mice were used. Fluorescent pictures were analyzed using Living Image software (XFL-MR filter; excitation: 570 nm; emission: 620 nm). Normal tissues and tumors were then collected, imaged, fixed in formalin and embedded in paraffin for H&E staining for further analysis. Blood was drawn from the heart, and sera were isolated and quantified for PEDF and TSP1.

For intra-tibial injection: 4×10^4 CL1–E10 or CL1–P15 cells in 2 μl were delivered into the proximal region of the tibia using a 27-gauge needle. In this study, SREs were defined by the appearance over time of clinical signs such as severe limping, significant fluorescent signal as determined by *in vivo* fluorescence bioimaging with osteolytic bone lesions (X-ray pictures) and pathological fractures. At the end point (emergence of SRE), bones were collected, decalcified, fixed, H&E stained and analyzed by a pathologist (BM) for the presence of tumor in the bone and the surrounding muscle. All protocols were approved by Texas Tech University Animal Care and Use Committee and were in agreement with the National Institute of Health's guidelines.

Microvessel density quantification. Tumor cryosections (5 μm thick) were analyzed for CD31 (specific marker for endothelial cells) as we described in the study by Filleur *et al.*[10] Cryosections were fixed for 10 min in acetone, 1:1 acetone/chloroform and acetone; and blocked with 2% donkey serum (Jackson ImmunoResearch, West Grove, PA, USA). The sections were then incubated with CD31 Ab (1/125, BD Pharmingen, San Jose, CA, USA) in 2% donkey serum, followed by donkey anti-rat rhodamine X (1/200, Jackson ImmunoResearch). Fluorescent images were obtained using a Zeiss LSM 510 MetaLaser Scanning confocal microscope and quantified with MetaView software. Microvessel density was defined as the average area corresponding to the CD31-positive structures counted in 10 high-powered fields per experiment condition.

Statistical evaluation of the data. Data are expressed as mean ± S.D. of three independent experiments, each done at least in triplicate. Statistical evaluation of the data was done using Student's *t*-test, one-way analysis of variance (ANOVA) or repeated measures ANOVA where appropriate (IBM SPSS Statistics 21 software, Armonk, NY, USA). *P*-values below 0.05 were considered statistically significant.

Conflict of Interest

The authors declare no conflict of interest.

1. Oudard S, Banu E, Beuzeboc P, Voog E, Dourthe LM, Hardy-Bessard AC et al. Multicenter randomized phase II study of two schedules of docetaxel, estramustine, and prednisone versus mitoxantrone plus prednisone in patients with metastatic hormone-refractory prostate cancer. *J Clin Oncol* 2005; **23**: 3343–3351.
2. Petrylak DP, Tangen CM, Hussain MH, Lara Jr PN, Jones JA, Taplin ME et al. Docetaxel and estramustine compared with mitoxantrone and prednisone for advanced refractory prostate cancer. *N Engl J Med* 2004; **351**: 1513–1520.
3. Tannock IF, de Wit R, Berry WR, Horti J, Pluzanska A, Chi KN et al. Docetaxel plus prednisone or mitoxantrone plus prednisone for advanced prostate cancer. *N Engl J Med* 2004; **351**: 1502–1512.
4. Mukherji D, Pezaro CJ, Shamseddine A, De Bono JS. New treatment developments applied to elderly patients with advanced prostate cancer. *Cancer Treat Rev* 2013; **39**: 578–583.
5. Filleur S, Nelius T, de Riese W, Kennedy RC. Characterization of PEDF: a multi-functional serpin family protein. *J Cell Biochem* 2009; **106**: 769–775.
6. Becerra SP. Structure-function studies on PEDF. A noninhibitory serpin with neurotrophic activity. *Adv Exp Med Biol* 1997; **425**: 223–237.
7. Dawson DW, Volpert OV, Gillis P, Crawford SE, Xu H, Benedict W et al. Pigment epithelium-derived factor: a potent inhibitor of angiogenesis. *Science* 1999; **285**: 245–248.
8. Doll JA, Stellmach VM, Bouck NP, Bergh AR, Lee C, Abramson LP et al. Pigment epithelium-derived factor regulates the vasculature and mass of the prostate and pancreas. *Nat Med* 2003; **9**: 774–780.
9. Halin S, Wikstrom P, Rudolfsson SH, Stattin P, Doll JA, Crawford SE et al. Decreased pigment epithelium-derived factor is associated with metastatic phenotype in human and rat prostate tumors. *Cancer Res* 2004; **64**: 5664–5671.
10. Filleur S, Volz K, Nelius T, Mirochnik Y, Huang H, Zaichuk TA et al. Two functional epitopes of pigment epithelial-derived factor block angiogenesis and induce differentiation in prostate cancer. *Cancer Res* 2005; **65**: 5144–5152.
11. Wilson C, Purcell C, Seaton A, Oladipo O, Maxwell PJ, O'Sullivan JM et al. Chemotherapy-induced CXC-chemokine/CXC-chemokine receptor signaling in metastatic prostate cancer cells confers resistance to oxaliplatin through potentiation of nuclear factor-kappaB transcription and evasion of apoptosis. *J Pharmacol Exp Ther* 2008; **327**: 746–759.
12. Wilson C, Scullin P, Worthington J, Seaton A, Maxwell P, O'Rourke D et al. Dexamethasone potentiates the antiangiogenic activity of docetaxel in castration-resistant prostate cancer. *Br J Cancer* 2008; **99**: 2054–2064.
13. Wilson C, Wilson T, Johnston PG, Longley DB, Waugh DJ. Interleukin-8 signaling attenuates TRAIL- and chemotherapy-induced apoptosis through transcriptional regulation of c-FLIP in prostate cancer cells. *Mol Cancer Ther* 2008; **7**: 2649–2661.
14. Smith ND, Schulze-Hoepfner FT, Veliceasa D, Filleur S, Shareef S, Huang L et al. Pigment epithelium-derived factor and interleukin-6 control prostate neuroendocrine differentiation via feed-forward mechanism. *J Urol* 2008; **179**: 2427–2434.
15. Hirsch J, Johnson CL, Nelius T, Kennedy R, Riese W, Filleur S. PEDF inhibits IL8 production in prostate cancer cells through PEDF receptor/phospholipase A2 and regulation of NFkappaB and PPARgamma. *Cytokine* 2011; **55**: 202–210.
16. Nelius T, Samathanam C, Martinez-Marin D, Gaines N, Stevens J, Hickson J et al. Positive correlation between PEDF expression levels and macrophage density in the human prostate. *Prostate* 2013; **73**: 549–561.
17. Halin S, Rudolfsson SH, Doll JA, Crawford SE, Wikstrom P, Bergh A. Pigment epithelium-derived factor stimulates tumor macrophage recruitment and is downregulated by the prostate tumor microenvironment. *Neoplasia* 2010; **12**: 336–345.
18. Sanagi T, Yabe T, Yamada H. The regulation of pro-inflammatory gene expression induced by pigment epithelium-derived factor in rat cultured microglial cells. *Neurosci Lett* 2005; **380**: 105–110.
19. Takanohashi A, Yabe T, Schwartz JP. Pigment epithelium-derived factor induces the production of chemokines by rat microglia. *Glia* 2005; **51**: 266–278.
20. Yabe T, Sanagi T, Schwartz JP, Yamada H. Pigment epithelium-derived factor induces pro-inflammatory genes in neonatal astrocytes through activation of NF-kappa B and CREB. *Glia* 2005; **50**: 223–234.
21. Zhang SX, Wang JJ, Gao G, Shao C, Mott R, Ma JX. Pigment epithelium-derived factor (PEDF) is an endogenous antiinflammatory factor. *FASEB J* 2006; **20**: 323–325.
22. Yoshida Y, Yamagishi SI, Matsui I, Nakamura K, Imaizumi T, Yoshimura K et al. Elevated levels of pigment epithelium-derived factor (PEDF) in aqueous humor of patients with uveitis. *Br J Ophthalmol* 2006; **91**: 149–150.
23. Eichler W, Yafai Y, Wiedemann P, Fengler D. Antievascular agents in the treatment of eye diseases. *Curr Pharm Des* 2006; **12**: 2645–2660.
24. Fontana A, Falcone A, Derosa L, Di Desidero T, Danesi R, Bocci G. Metronomic chemotherapy for metastatic prostate cancer: a 'young' concept for old patients? *Drugs Aging* 2010; **27**: 689–696.
25. Emmenegger U, Francia G, Shaked Y, Kerbel RS. Metronomic chemotherapy: principles and lessons learned from applications in the treatment of metastatic prostate cancer. *Recent Results Cancer Res* 2010; **180**: 165–183.
26. Nelius T, Rinard K, Filleur S. Oral/metronomic cyclophosphamide-based chemotherapy as option for patients with castration-refractory prostate cancer: review of the literature. *Cancer Treat Rev* 2011; **37**: 444–455.
27. Fontana A, Galli L, Fioravanti A, Orlandi P, Galli C, Landi L et al. Clinical and pharmacodynamic evaluation of metronomic cyclophosphamide, celecoxib, and

dexamethasone in advanced hormone-refractory prostate cancer. *Clin Cancer Res* 2009; **15**: 4954–4962.

28. Bocci G, Francia G, Man S, Lawler J, Kerbel RS. Thrombospondin 1, a mediator of the antiangiogenic effects of low-dose metronomic chemotherapy. *Proc Natl Acad Sci USA* 2003; **100**: 12917–12922.

29. Damber JE, Vallbo C, Albertsson P, Lennernas B, Norrby K. The anti-tumour effect of low-dose continuous chemotherapy may partly be mediated by thrombospondin. *Cancer Chemother Pharmacol* 2006; **58**: 354–360.

30. Quesada AJ, Nelius T, Yap R, Zaichuk TA, Alfranca A, Filleur S et al. In vivo upregulation of CD95 and CD95L causes synergistic inhibition of angiogenesis by TSP1 peptide and metronomic doxorubicin treatment. *Cell Death Differ* 2005; **12**: 649–658.

31. Yap R, Veliceasa D, Emmenegger U, Kerbel RS, McKay LM, Henkin J et al. Metronomic low-dose chemotherapy boosts CD95-dependent antiangiogenic effect of the thrombospondin peptide ABT-510: a complementation antiangiogenic strategy. *Clin Cancer Res* 2005; **11**: 6678–6685.

32. Shaked Y, Emmenegger U, Francia G, Chen L, Lee CR, Man S et al. Low-dose metronomic combined with intermittent bolus-dose cyclophosphamide is an effective long-term chemotherapy treatment strategy. *Cancer Res* 2005; **65**: 7045–7051.

33. Wada S, Yoshimura K, Hipkiss EL, Harris TJ, Yen HR, Goldberg MV et al. Cyclophosphamide augments antitumor immunity: studies in an autochthonous prostate cancer model. *Cancer Res* 2009; **69**: 4309–4318.

34. Lutsiak ME, Semnani RT, De Pascalis R, Kashmiri SV, Schlom J, Sabzevari H. Inhibition of CD4(+)25+ T regulatory cell function implicated in enhanced immune response by low-dose cyclophosphamide. *Blood* 2005; **105**: 2862–2868.

35. Raghavan D, Cox K, Pearson BS, Coorey GJ, Rogers J, Watt WH et al. Oral cyclophosphamide for the management of hormone-refractory prostate cancer. *Br J Urol* 1993; **72**(Pt 1): 625–628.

36. Nelius T, Klatte T, de Riese W, Haynes A, Filleur S. Clinical outcome of patients with docetaxel-resistant hormone-refractory prostate cancer treated with second-line cyclophosphamide-based metronomic chemotherapy. *Med Oncol* 2010; **27**: 363–367.

37. Koletsky AJ, Guerra ML, Kronish L. Phase II study of vinorelbine and low-dose docetaxel in chemotherapy-naive patients with hormone-refractory prostate cancer. *Cancer J* 2003; **9**: 286–292.

38. Krainer M, Tomek S, Elandt K, Horak P, Albrecht W, Eisenmenger M et al. A prospective, open label, randomized phase II trial of weekly docetaxel versus weekly vinorelbine as first line chemotherapy in patients with androgen independent prostate cancer. *J Urol* 2007; **177**: 2141–2145; discussion 2145.

39. Cumashi A, Tinari N, Rossi C, Lattanzio R, Natoli C, Piantelli M et al. Sunitinib malate (SU-11248) alone or in combination with low-dose docetaxel inhibits the growth of DU-145 prostate cancer xenografts. *Cancer Lett* 2008; **270**: 229–233.

40. Reiner T, de las Pozas A, Gomez LA, Perez-Stable C. Low dose combinations of 2-methoxyestradiol and docetaxel block prostate cancer cells in mitosis and increase apoptosis. *Cancer Lett* 2009; **276**: 21–31.

41. Hasegawa M, Miyajima A, Kosaka T, Yasumizu Y, Tanaka N, Maeda T et al. Low-dose docetaxel enhances the sensitivity of S-1 in a xenograft model of human castration resistant prostate cancer. *Int J Cancer* 2012; **130**: 431–442.

42. Bastatas L, Martinez-Marin D, Matthews J, Hashem J, Lee YJ, Sennoune S et al. AFM nano-mechanics and calcium dynamics of prostate cancer cells with distinct metastatic potential. *Biochim Biophys Acta* 2012; **1820**: 1111–1120.

43. Klement G, Baruchel S, Rak J, Man S, Clark K, Hicklin DJ et al. Continuous low-dose therapy with vinblastine and VEGF receptor-2 antibody induces sustained tumor regression without overt toxicity. *J Clin Invest* 2000; **105**: R15–R24.

44. Man S, Bocci G, Francia G, Green SK, Jothy S, Hanahan D et al. Antitumor effects in mice of low-dose (metronomic) cyclophosphamide administered continuously through the drinking water. *Cancer Res* 2002; **62**: 2731–2735.

45. Singh RK, Lokeshwar BL. Depletion of intrinsic expression of Interleukin-8 in prostate cancer cells causes cell cycle arrest, spontaneous apoptosis and increases the efficacy of chemotherapeutic drugs. *Mol Cancer* 2009; **8**: 57.

46. Mita AC, Figlin R, Mita MM. Cabazitaxel: more than a new taxane for metastatic castrate-resistant prostate cancer? *Clin Cancer Res* 2012; **18**: 6574–6579.

47. Oudard S. Progress in emerging therapies for advanced prostate cancer. *Cancer Treat Rev* 2013; **39**: 275–289.

48. Scosyrev E, Messing EM, Mohile S, Golijanin D, Wu G. Prostate cancer in the elderly: frequency of advanced disease at presentation and disease-specific mortality. *Cancer* 2012; **118**: 3062–3070.

49. Campbell LM, Maxwell PJ, Waugh DJ. Rationale and means to target pro-inflammatory interleukin-8 (CXCL8) signaling in cancer. *Pharmaceuticals* 2013; **6**: 929–959.

50. Emmenegger U, Francia G, Chow A, Shaked Y, Kouri A, Man S et al. Tumors that acquire resistance to low-dose metronomic cyclophosphamide retain sensitivity to maximum tolerated dose cyclophosphamide. *Neoplasia* 2011; **13**: 40–48.

51. Chow A, Wong A, Francia G, Man S, Kerbel RS, Emmenegger U. Preclinical analysis of resistance and cross-resistance to low-dose metronomic chemotherapy. *Invest New Drugs* 2013; **32**: 47–59.

52. Wang L, Huang X, Zheng X, Wang X, Li S, Zhang L et al. Concurrent chemoradiotherapy with low-dose docetaxel inhibits the growth of DU-145 prostate cancer xenografts. *Clin Transl Oncol* 2013; e-pub ahead of print 9 October 2013.

53. Jia L, Waxman DJ. Thrombospondin-1 and pigment epithelium-derived factor enhance responsiveness of KM12 colon tumor to metronomic cyclophosphamide but have disparate effects on tumor metastasis. *Cancer Lett* 2013; **330**: 241–249.

54. Chen J, Ye L, Zhang L, Jiang WG. The molecular impact of pigment epithelium-derived factor, PEDF, on lung cancer cells and the clinical significance. *Int J Oncol* 2009; **35**: 159–166.

55. Ek ET, Dass CR, Contreras KG, Choong PF. Pigment epithelium-derived factor overexpression inhibits orthotopic osteosarcoma growth, angiogenesis and metastasis. *Cancer Gene Ther* 2007; **14**: 616–626.

56. Orgaz JL, Ladhani O, Hoek KS, Fernandez-Barral A, Mihic D, Aguilera O et al. 'Loss of pigment epithelium-derived factor enables migration, invasion and metastatic spread of human melanoma'. *Oncogene* 2009; **28**: 4147–4161.

57. Uehara H, Miyamoto M, Kato K, Ebihara Y, Kaneko H, Hashimoto H et al. Expression of pigment epithelium-derived factor decreases liver metastasis and correlates with favorable prognosis for patients with ductal pancreatic adenocarcinoma. *Cancer Res* 2004; **64**: 3533–3537.

58. Tso CL, McBride WH, Sun J, Patel B, Tsui KH, Paik SH et al. Androgen deprivation induces selective outgrowth of aggressive hormone-refractory prostate cancer clones expressing distinct cellular and molecular properties not present in parental androgen-dependent cancer cells. *Cancer J* 2000; **6**: 220–233.

59. Teicher BA. Tumor models for efficacy determination. *Mol Cancer Ther* 2006; **5**: 2435–2443.

60. Mohammad RM, Wall NR, Dutcher JA, Al-Katib AM. The addition of bryostatin 1 to cyclophosphamide, doxorubicin, vincristine, and prednisone (CHOP) chemotherapy improves response in a CHOP-resistant human diffuse large cell lymphoma xenograft model. *Clin Cancer Res* 2000; **6**: 4950–4956.

Supplementary Information accompanies this paper on Cell Death and Disease website (http://www.nature.com/cddis)